JOURNAL OF CATALYSIS **162,** 190–197 (1996)
ARTICLE NO. 0276

Surface Characteristics and Activity of Chromia/Alumina Catalysts Prepared by Atomic Layer Epitaxy

Arla Kytökivi,*,[1] Jean-Paul Jacobs,†,[2] Arja Hakuli,*,‡ Jouni Meriläinen,*,§ and Hidde H. Brongersma†

*Microchemistry Ltd., P.O. Box 45, FIN-02151 Espoo, Finland; †Faculty of Physics and Schuit Institute of Catalysis, Eindhoven University of Technology, P.O. Box 513, 5600 MB Eindhoven, The Netherlands; ‡Department of Chemical Engineering, Helsinki University of Technology, Kemistintie 1, FIN-02151 Espoo, Finland; and §Laboratory of Analytical Chemistry, Department of Chemistry, University of Helsinki, P.O. Box 55, FIN-00014 University of Helsinki, Finland

Received July 20, 1995; revised April 2, 1996; accepted April 30, 1996

A series of CrO_x/γ-Al_2O_3 catalysts was prepared by atomic layer epitaxy (ALE) from the vapor phase, with use of sequential saturating reactions of $Cr(acac)_3$ vapor and air. The loading was varied from 1.3 to 8.8 wt% of Cr. Lower loadings were achieved by partially blocking the alumina surface with acetylacetone or dipivaloylmethane before introducing $Cr(acac)_3$. The catalytically active material was found to be evenly distributed through the catalyst particles. Low energy ion scattering measurements showed that, up to 7.4 wt% of Cr, the Cr species was dispersed in a monolayer. XPS and UV-vis spectrophotometry revealed that, even at the low loadings, both Cr^{3+} and Cr^{6+} species were present. This was attributed to a stabilization of Cr^{3+} on the alumina support during the ALE process. Loading beyond monolayer coverage was not reflected in the dehydrogenation of *i*-butane to *i*-butene: the activity continued to increase.

INTRODUCTION

Chromia/alumina catalysts possess high activity and selectivity in the dehydrogenation of light alkanes such as propane and butane (1). The catalysts were studied intensively in the 1950s and 1960s (1) and recent studies show that the interest continues (2–19). In most of these studies the catalysts have been prepared by impregnation using CrO_3 or $Cr(NO_3)_3$ as precursor. In contrast to this, the chromia/alumina catalysts of the present work were prepared by atomic layer epitaxy (ALE) with the use of sequential saturating reactions of $Cr(acac)_3$ vapor and air.

ALE is a gas-phase technique, the use of which has been expanded from thin film growth to the preparation of catalysts (20–22). Already it shows great promise in the preparation of tailored catalysts. ALE is distinguished from the chemical vapor deposition techniques in the use of saturating gas–solid reactions to form the required surface. These saturating and self-terminating reactions ensure a uniform distribution of the chemisorbed species throughout the porous catalyst support. The surface of the support and the reagent selected determine the density of the surface species during each reaction step. The concentration of the desired component is not dependent on the dose of the reactant provided that the dose exceeds the amount required for surface saturation. Thus, the earlier work of Köhler *et al.* (16, 17) using $Cr(acac)_3$ vapor in the preparation of catalysts differs from the ALE technique because the concentration of chromium was there controlled by regulating the contact time between $Cr(acac)_3$ and oxide supports in a fluidized bed and not only through the use of saturating reactions.

The aim of our work was to study the growth of chromia on γ-alumina during the preparation of chromia/alumina catalysts from vapor phase by ALE and to explore the relationship between the surface species and the behavior of the catalysts in the dehydrogenation of *i*-butane to *i*-butene. Accordingly, a series of catalysts with various Cr loadings was prepared and the macroscopic homogeneity of these samples was confirmed by electron microscopy, XRD, and surface area/porosity measurements. A more detailed investigation of the surface was performed by low energy ion scattering (LEIS) and XPS. In this way we were able to monitor the growth process and the nature of the Cr species on the alumina support during the ALE preparation. Our findings on the CrO_x/γ-Al_2O_3 system are compared with those of earlier work on NiO/γ-Al_2O_3 (23, 24) and CrO_x/SiO_2 (25, 26) systems prepared by ALE using $Ni(acac)_2$ and $Cr(acac)_3$ vapors. Finally, the series of CrO_x/γ-Al_2O_3 catalysts was tested in the dehydrogenation of *i*-butane to *i*-butene.

EXPERIMENTAL

Catalyst Preparation

The support material was γ-alumina (000-1.5E) from Akzo Nobel. The support was crushed to a particle size

[1] Corresponding author. E-mail: Arla.Kytokivi@microchem.fi; tel: +358-204505704; fax: +358-204505700.

[2] Present address: Philips Components B.V., Display Components Eindhoven, P.O. Box 218, 5600 MD Eindhoven, The Netherlands.

0021-9517/96 $18.00

of 0.2–0.4 mm or 0.7–1.0 mm. The values of specific surface area and pore volume for the uncalcined material were 195 m^2/g and 0.49 cm^3/g, respectively. $Cr(acac)_3$, i.e., $Cr(C_5O_2H_7)_3$, was 99% pure and purchased from Riedel-de Haën. Synthetic air was used for the removal of the ligands. Acetylacetone ($C_5H_8O_2$, Hacac) from Merck and dipivaloylmethane ($C_{11}H_{20}O_2$, Hthd) from Fluka were used as blocking agents.

The support material (4–10 g) was preheated for 16 h in a muffle furnace at 600°C, and then the preheat treatment was continued at 200°C for 3 h in a fixed-bed flow-type reactor (24) (Microchemistry Ltd.) under a pressure of 5–10 kPa in nitrogen flow. The solid $Cr(acac)_3$ was vaporized at 190°C, and then was transported, in nitrogen, downwards through the solid support bed. The reaction of $Cr(acac)_3$ was carried out at 200°C. This reaction sequence was followed by a nitrogen purge for at least 2 h at the reaction temperature. To remove the ligand residues from the samples, air treatment was started at 200°C and continued at 600°C for 3–4 h. The high preheat and air treatment temperatures used in the preparation were chosen to correspond to the conditions in the dehydrogenation reaction. To increase the Cr concentration of the samples, the $Cr(acac)_3$, nitrogen, and air sequences were repeated between one and seven times. To decrease the Cr concentration, Hacac or Hthd was bound to the surface at 200°C, followed by nitrogen purge at 200°C, before the introduction of $Cr(acac)_3$ to the reactor. Hacac and Hthd were vaporized at 60°C and 80°C, respectively. The amount of $Cr(acac)_3$, Hacac, or Hthd vaporized was always kept sufficiently high to ensure surface saturation.

Catalyst Characterization

The carbon content after $Cr(acac)_3$ adsorption was determined with a Leco CR12 carbon analyzer. The Cr concentration was measured by instrumental neutron activation analysis (INAA). Cr^{6+} concentration, after ligand removal, was determined in basic solution as chromate by UV-vis spectrophotometry (27). The samples were heated in a muffle furnace in air at 600°C for 1 h before the dissolution of the Cr^{6+} species. To check the influence of the heating step on the Cr^{6+} concentration, the Hacac-blocked sample and the samples with a loading of one and seven ALE cycles were subjected to heat treatment of 16 h at 500°C in air before dissolution. The Cr concentration of the catalysts is given as wt% of Cr metal or as number of Cr atoms per nm^2 (Cr/nm^2), where an average specific surface area of 190 m^2/g was used for the computation.

Specific surface areas and pore volumes were determined by means of nitrogen adsorption and condensation using Micromeritics ASAP 2400 equipment (BET-method). X-ray diffraction (XRD) measurements were made with Siemens Diffrac 500 diffractometer and Cu$K\alpha$ radiation. For scanning electron microscopy (SEM) examination, the sample particles were embedded in epoxy resin and the cured block was cut with a microtome until a sufficient number of cross-sectioned particles were exposed in the block face. All samples were coated with carbon to prevent charging under the electron beam. The examination was carried out with a Jeol JSM 840A scanning electron microscope fitted with a PGT IMIX III energy dispersive X-ray (EDS) and image analyzer. The accelerating voltage used in SEM examinations was 15 keV.

X-ray photoelectron (XPS) spectra were measured with an X-probe model 101 spectrometer (Surface Science Instruments, VG Fisons) equipped with a monochromatized Al$K\alpha$ X-ray source. The instrument was operated at 10 kV and 12 mA in the constant pass energy (50 eV) mode using a spot size of 600 μm. With these settings and a step width of 80 meV/channel, the FWHM value for Au $4f_{7/2}$ was 1.05 eV. After being cooled in flowing nitrogen in the ALE reactor, the samples were inertly transferred to the instrument. During the XPS analysis, Cr^{6+} reduction in the sample chamber was minimized by use of a short analysis time. All binding energies were referenced to the Al 2p signal for Al_2O_3 at 74.5 eV. The relative surface concentrations for the elements of interest were calculated from the Cr $2p_{3/2}$, Al 2p, and O 1s signal intensities, using atomic sensitivity factors provided by the instrument manufacturer. The small amount of carbon, which was observed in all samples, was not taken into account in the calculations. The base pressure during data acquisition was below 4×10^{-6} Pa.

Low-energy ion scattering (LEIS) measurements were made with a NODUS instrument. For a description of its basic design, as it is used today, and a review of the application of the LEIS technique to oxides, the reader is referred to Ref. (28). The primary $^4He^+$ ions (3 keV) are generated in a Leybold IQE 12/38 source and are directed perpendicularly onto the target. To keep the exposure of the sample below 10^{13} ions/cm^2 the ion flux was kept low. Ions scattered over 142° are energy selected by a modified cylindrical mirror analyzer (CMA). Charging of the insulating materials can be effectively compensated for by flooding from all sides with low-energy electrons. The base pressure is in the low 10^{-6} Pa, which increases during the operation of the ion beam to the high 10^{-6} Pa. This is due to the inert gas of the ion beam, which will not influence the analysis results. All catalyst powders were pressed into wafers in an ambient atmosphere and, before analysis, chemically cleaned in a calcination step at 200°C in 3 kPa of oxygen in a connecting chamber.

Activity Measurements

The activity of the catalysts was studied in the dehydrogenation of *i*-butane at atmospheric pressure at 540°C in a fixed bed flow reactor (diameter 9 mm). The catalyst charge was 200 mg and the particle size of the catalyst

0.2–0.4 mm. Before testing, the catalysts were calcined *in situ* with synthetic air at 600°C for 16 h, and then reduced with hydrogen (1:10 in nitrogen) at 540°C for 0.5 h; *i*-butane, diluted with nitrogen (1:10), was used as feed. The total flow rate was 200 cm^3/min (STP) during both reduction and reaction. The product distribution was monitored with an on-line FT-IR analyzer. Spectra were measured for 1 s at time intervals of 8 s. The multicomponent method used in the analysis of the measured IR spectra has been described in detail elsewhere (29, 30); *i*-butene along with some cracking and isomerization products were detected in the product flows. The activity is expressed as a mean of the conversions measured during the time period of 30–60 s on stream. Thus, the results describe the initial activity, to avoid problems associated with deactivation of the catalysts.

RESULTS

Catalyst Preparation

The first ALE sequence of $Cr(acac)_3$ led to a sample containing 1.3 wt% of Cr. This corresponded to a saturation density of 0.8 Cr/nm^2. The carbon concentration of the sample was determined before ligand removal to study the binding of $Cr(acac)_3$ to the surface. The value of 3.4 wt% C, giving a C/Cr ratio of 11, implied that one ligand was released in the surface reaction, leaving two ligands bound to the chromium center. To form the final oxide surface the ligands were removed by heating the sample in air at 600°C. During this treatment the color of the sample changed from green to yellow, indicating that Cr^{3+} had become oxidized to Cr^{6+} species. To study the catalysts at lower Cr loadings, the $Cr(acac)_3$ sequence was preceded by a saturating sequence of Hthd or Hacac. In this way, part of the surface was effectively blocked for $Cr(acac)_3$, resulting in samples of 0.16 and 0.32 wt% Cr with Hacac and Hthd, respectively (Table 1). The use of blocking agents for this kind of atomic engineering with ALE has earlier been described by Haukka *et al.* (25).

When the ALE sequences of $Cr(acac)_3$ at 200°C and air at 600°C were repeated for a total of seven times, the Cr loading of the catalysts was increased from 1.3 wt% to 8.8 wt% (Table 1). As Fig. 1 shows, the loading increased linearly with the number of cycles. The same was found earlier for the NiO/γ-alumina system prepared by ALE with $Ni(acac)_2$ and air (24). The results indicate that about the same amount of chromium was bound to the surface after each $Cr(acac)_3$ sequence. The color of the samples changed from yellow to dark brown with increasing chromium concentration. The average surface densities of the highest loadings, 7.4 wt% and 8.8 wt% were 4.5 and 5.4 Cr/nm^2, respectively. These values exceeded the monolayer coverage of impregnated chromia/γ-alumina catalysts of 3.7 Cr/nm^2 reported by Wachs *et al.* (7).

TABLE 1

Cr and Cr^{6+} Concentrations, Surface Areas, and Pore Volumes of CrO_x/γ-Al_2O_3 Catalysts

Number of $Cr(acac)_3$ and air cycles	Cr (wt%)	Cr^{6+} UV-vis (wt%)	Cr^{6+} UV-vis (%)	Cr^{6+} XPS (%)	Surface area (m^2/g)	Pore volume (cm^3/g)
Support	—	—	—	—	195	0.49
1/Hacac-blocked	0.16	0.13	81	—	—	—
1/Hthd-blocked	0.32	0.26	81	—	—	—
1	1.3	1.0	77	66	200	0.49
2	2.5	1.6	64	66	—	—
3	3.7	2.2	59	63	195	0.47
4	5.0	2.4	48	45	—	—
5	6.5	2.6	40	50	—	—
6	7.4	2.7	36	40	185	0.42
7	8.8	2.7	31	38	185	0.42

The valence state distribution of Cr^{6+} and Cr^{3+} as a function of loading was determined by measuring the Cr^{6+} content by UV-vis spectrophotometry and assuming that only Cr^{3+} and Cr^{6+} were present in the oxidized catalysts. The results are shown in Fig. 1 and Table 1; Cr^{3+} was observed in all samples. The amount of Cr^{6+} in the samples increased during the first cycles but leveled off in the two samples with the highest Cr concentration. In view of the report of Vuurman *et al.* (3) that Cr can be fully oxidized to Cr^{6+} up to a monolayer coverage, a calcination at 500°C for 16 h was applied to the catalysts with loadings of 0.16 wt%, 1.3 wt%, and 8.8 wt%. However, this longer heat treatment in air at a lower temperature did not increase the Cr^{6+} concentration measured by UV-vis spectrophotometry, indicating a high stability or Cr^{3+} species.

Although all the catalysts had a homogeneous appearance with respect to color, they were examined by SEM to verify that chromium had penetrated into the heart of the

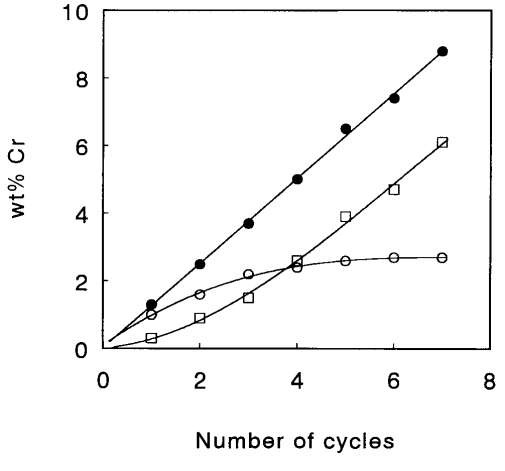

FIG. 1. Chromium concentration of the catalysts as a function of the number of ALE reaction cycles: ●, total Cr; ○, Cr^{6+}; □, Cr^{3+}.

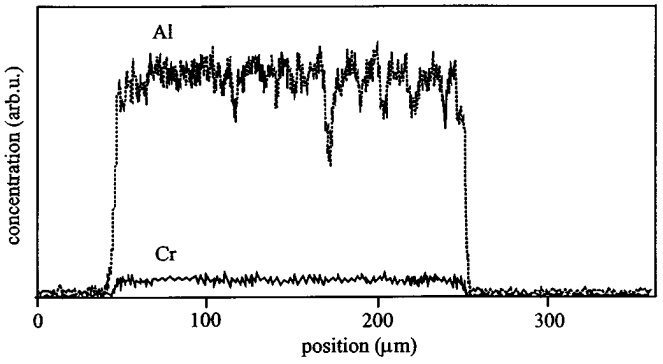

FIG. 2. EDS line scan across a cross-sectioned particle surface after seven $Cr(acac)_3$ and air cycles (8.8 wt% Cr).

support particles. With back-scattered imaging mode, the color of the particles on the gray scale was observed to be even, indicating uniform Cr concentration. Furthermore, EDS line scans across the cross-sectioned particle surfaces confirmed that chromium was evenly distributed through the particles. An example of the Cr loading measured by EDS is shown in Fig. 2.

The specific surface areas and pore volumes are listed in Table 1. The results show that the surface area of alumina was maintained since the decrease in the values corresponded to the weight increase of the catalysts calculated as CrO_3; XRD measurements provided no evidence of formation of an α-Cr_2O_3 or other chromium phase. We conclude, therefore, that the ALE preparation resulted in catalysts where the catalytically active material was distributed homogeneously through the catalyst.

Surface Characterization

To obtain a more detailed picture of the chromium dispersion at the atomic level, we carried out surface analysis by XPS and LEIS. LEIS is more surface sensitive, probing only the topmost atomic layer (28), while XPS provides chemical information in addition to the surface composition. In both techniques it is assumed that the external surface is a good representation of the internal surface.

The Cr $2p_{3/2}$ signal was used in the XPS measurements to calculate the relative Cr concentration. This signal was found to increase steadily as a function of Cr concentration of the samples as depicted in Fig. 3. The Al 2p signals decreased slightly, while the O 1s signal was constant. Furthermore, after grinding the 7.4 wt% sample, the XPS measurements showed, within experimental error, no deviation from the unground sample, confirming the good homogeneity of the catalysts.

The relative abundance of Cr^{3+} and Cr^{6+} in the samples was determined by deconvoluting the Cr $2p_{3/2}$ signal. Symmetric Gaussian components and a Shirley background were employed. For Cr^{3+} and its satellite we applied constraints close to the reported values (31). An example of

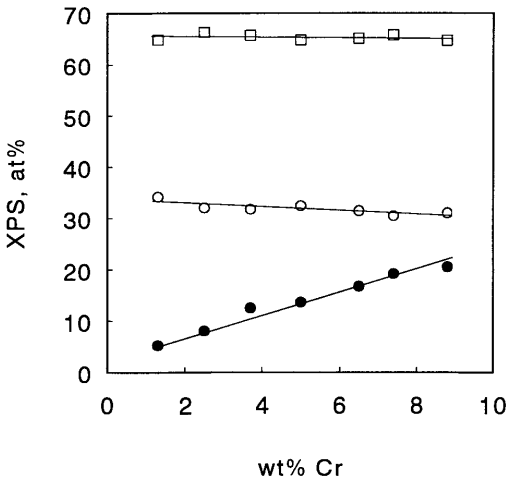

FIG. 3. XPS results in atomic percent: ●, chromium; ○, aluminum; □, oxygen for various chromium loadings. The intensities of the chromium signals in the figure have been multiplied by 5.

the deconvolution is given in Fig. 4. The amount of Cr^{6+} in the inertly transferred samples was in agreement with the UV-vis spectrophotometric measurements of samples exposed to ambient conditions and extra heating at 600°C for 1 h (Table 1). The binding energy values measured by XPS, of 577.2 ± 0.2 eV for Cr^{3+} and 579.8 ± 0.3 eV for Cr^{6+}, corresponded well with the values reported by Grünert *et al.* (31) and by Rahman *et al.* (15) for chromia/alumina catalysts.

The results of the LEIS experiments are displayed in Figs. 5 and 6. A light ion ($^4He^+$) was used for the analysis, and the ion flux on the sample was kept as low as possible by measuring only the interval of interest. Time-dependent measurements showed that the influence of damage by the ion beam on the data could be neglected. The spectra were calibrated to the oxygen signals, on the assumption that the oxygen signals were constant for the loadings studied. This

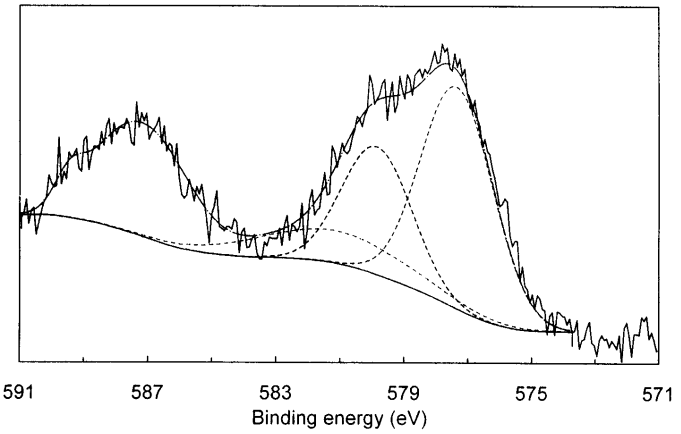

FIG. 4. Example of a Cr 2p spectrum for an 8.8 wt% Cr sample. Peak fitting inserted for the Cr $2p_{3/2}$ region showing components, from left to right, for Cr^{3+} satellite, Cr^{6+} and Cr^{3+}.

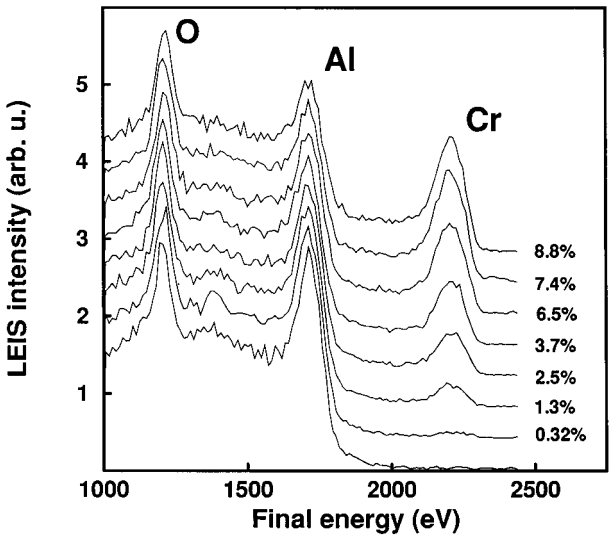

FIG. 5. LEIS spectra of the series CrO_x/γ-Al_2O_3 catalysts.

has been proven valid for a number of systems (19, 23, 32). The ratios were determined in three different ways: with peak heights, peak areas after linear background subtraction, and peak areas. A semi-empirical model introduced by Nelson (33) and adapted for our purposes was used (34). All three methods showed the same trend and the average was taken for Fig. 6. The intensity of the Cr signal increased linearly up to a loading of about 7.5 wt% Cr, after which a slowing of the rate of increase indicated multilayer growth. The LEIS results show that, with ALE, a monolayer coverage was reached at about 4.5 Cr/nm^2.

Activity in Dehydrogenation of i-Butane

Figure 7 depicts the initial activity of the catalysts after prereduction in H_2, expressed as conversion of *i*-butane.

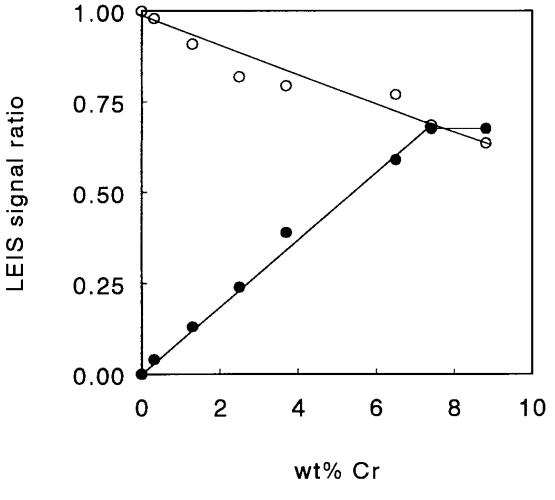

FIG. 6. Normalized Cr and Al intensities determined by LEIS measurements of the CrO_x/γ-Al_2O_3 catalysts: ○, Al/O; ●, Cr/O.

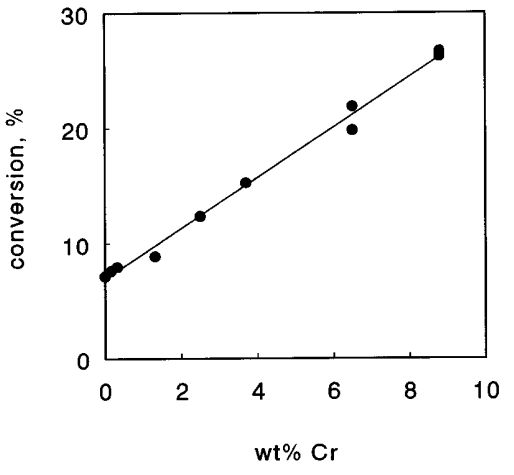

FIG. 7. Initial activity of chromia/alumina catalysts in dehydrogenation of *i*-butane after prereduction in H_2.

The results describe an increase in activity with chromium loading, from the low loadings where isolated CrO_x species are assumed to exist even after reduction, to monolayer coverage and even above.

In the interpretation of the results, note that the reported activity includes cracking and isomerization, which occurred in addition to dehydrogenation. Both alumina and chromium oxide surface may be involved in these side reactions. On pure alumina, conversion was 7% and selectivity for *i*-butene 43%. On chromium oxide catalysts, the selectivity for *i*-butene increased with Cr loading to 91%. However, a level of 90% was achieved rapidly, at Cr loadings as low as 1.3–2.5 wt%.

DISCUSSION

Dispersion of Chromia/Alumina Prepared by ALE

ALE is based on the use of saturating self-terminating gas-solid reactions. In the case of $Cr(acac)_3$ on γ-alumina, the saturation level under the reaction conditions used was 0.8 Cr/nm^2. On the basis of the carbon content measured after a single sequence of $Cr(acac)_3$ it seemed that one of the acac ligands was released when the molecule was bound to the surface. These results agree well with the earlier ALE work with β-diketonates on silica, where a similar saturation density of $Cr(acac)_3$ of 0.8/nm^2 was found. There, too, one of the ligands of the $Cr(acac)_3$ was released (25, 26). In the ALE process of $Ni(acac)_2$ on alumina, a saturation level of 2.0 Ni/nm^2 was reported. In that case, however, the acac/Ni ratio of the surface complex was one, which means that more Ni was deposited per ALE cycle (24).

The running of sequential reactions gave us a series of samples in which the concentration increased linearly, indicating that the saturation level was the same for each cycle. This linear behavior is not a self-evident property of the ALE method, since the surface changes after every ALE

cycle; instead, it is a property of the reagent/support combination in question. Apparently in the $Cr(acac)_3$/alumina system the steric hindrance by the acac groups, and not the limited number of bonding sites, determined the saturation level. The work of Haukka *et al.* (25) has shown that the adsorption of $Cr(acac)_3$ on silica occurs selectively through reaction with OH groups. Probably OH groups behave as bonding sites on alumina as well, at least during the first sequences of $Cr(acac)_3$. In addition, the adsorption of $Cr(acac)_3$ to coordinatively unsaturated aluminum and oxygen atoms, i.e., to Lewis sites, present on dehydroxylated alumina cannot be ruled out. Bonding solely through OH groups would require the formation of new OH groups during the air treatment after the $Cr(acac)_3$ sequence, because the original OH density of 600°C alumina is lower than the Cr surface density achieved after the cycle runs. Furthermore, the growth of CrO_x on top of CrO_x species from earlier cycles was excluded in the LEIS measurements.

Indeed, the linear increase of the LEIS signals from the lowest loadings (0.16 wt% and 0.32 wt%), where an atomic dispersion was guaranteed by the use of blocking agents, to a loading of 7.4 wt% after six ALE cycles, indicated a dispersion of the Cr species until a monolayer coverage was reached at about 4.5 Cr/nm^2. The highest loading showed no further increase of the LEIS signal, pointing to multilayer growth. XPS confirmed the homogeneous deposition of the Cr species, together with SEM/EDS and surface area measurements, and XRD gave no evidence of the formation of any crystalline chromia phases. Evidently, owing to the controlled binding of Cr on the alumina surface in the ALE process, a higher coverage can be reached than by conventional impregnation techniques where, above a surface concentration of about 4 Cr/nm^2, agglomeration occurs (3).

As revealed by the LEIS measurements, the ALE growth of CrO_x on alumina differs from that of NiO (23), although in both systems an acetylacetonate compound was the precursor for the deposition of the catalytically active species. In both systems an atomically dispersed species formed on the alumina support during the first ALE sequence. However, whereas the growth of $Ni(acac)_2$ on nickel oxide during the second ALE cycle, $Cr(acac)_3$ preferred bonding to the alumina in up to six reaction cycles.

Oxidation State of Cr in Chromia/Alumina

In the discussion thus far, the ALE catalysts have been seen to exhibit similar behavior to conventional impregnated catalyst, namely a monolayer formation. The only significant difference was the higher monolayer coverage for the ALE catalysts. When the growth mechanism was considered in the light of the oxidation states of chromium, however, a different picture emerged of the ALE catalysts.

It is generally accepted that, on calcined catalysts at low loadings, the chromium is anchored on the alumina surface as Cr^{6+} (e.g., 3, 8, 12, 19, 35). For higher loadings, opinions about the valence state distribution of the chromia are divided, probably because samples are not always prepared in the same way and possibly also because different characterization techniques are employed in the determination of oxidation states. For example, Vuurman *et al.* (3) report that up to a monolayer (4 Cr/nm^2), all the chromium oxide species are stabilized in oxidation state 6+ on the alumina support at moderate calcination temperatures ($\leq$500°C). In contrast, Kozłowski (36) reports that only 60% of Cr is in oxidation state 6+ at a monolayer coverage (3.9 Cr/nm^2). Rahman *et al.* (15) found Cr^{3+} at the same loadings, citing calcination-induced reduction of Cr^{6+} due to relatively high calcination temperatures of 600°C as an explanation. Above monolayer coverage the picture is consistent: Cr^{3+} is always found in the samples. This occurrence of Cr^{3+} is related to the formation of α-Cr_2O_3 and, according to Fouad *et al.* (11), in part to the presence of highly dispersed Cr^{3+} species.

In contrast to literature reports, we detected Cr^{3+} in our ALE catalysts even at low loadings of the samples. The same results were obtained by UV-vis spectrophotometry and XPS. Furthermore, although the amount of Cr^{6+} increased with the loading, even at a monolayer coverage only 35% of the Cr occurred as Cr^{6+}. The formation of Cr^{3+} in our case may be related to the high state of dehydroxylation of alumina, but still the monolayer structure is maintained. The role of hydroxyl groups in stabilizing the monolayer and different chromate structures (Cr^{6+} in mono-, di- and polychromates) has been emphasized in the literature. Both Turek *et al.* (6) and Vuurman *et al.* (4) argue that the increase in the chromium concentration up to monolayer coverage can be linked to the consumption of the alumina OH groups. Wachs *et al.* (7) more generally propose that monolayer coverage is unique for each transition metal/support pair, with the determining factor being the surface hydroxyl chemistry of the support. In their study of Cr on SiO_2, SiO_2–Al_2O_3, and Al_2O_3, Weckhuysen *et al.* (10) explain the Cr dispersion on the different supports in terms of the amount and characteristics of the hydroxyl groups. The more OH groups available, the better the dispersion. Also, Fouad *et al.* (11) argue that the high surface OH density on alumina prevents the polymerization of surface CrO_x species to α-Cr_2O_3 bulk phase and thus ensures the stability of dispersed high valence species.

In addition to studies on valence state distribution after the first calcination after impregnation, the chromia /alumina system has been studied intensively after reduction/recalcination processes. Weckhuysen *et al.* (8–10) investigated chromia/alumina catalysts of 0.2–0.8 wt% of Cr showing only chromate species on the surface after calcination at 720°C and 550°C. Upon reduction with CO, these Cr^{6+} species were reduced to Cr^{3+}, with further reduction to Cr^{2+} being mainly prevented by a stabilizing

effect of the alumina. They proposed that part of the Cr^{3+} is incorporated in the vacant octahedral sites of the spinel surface. Diffusion into these vacant Al^{3+} sites is facilitated by the similar ionic radii and charge of Cr^{3+} and Al^{3+} (9). Alternatively, the authors suggest on the basis of ^{27}Al MAS NMR measurements that Cr^{3+} occupies sites on alumina in the close vicinity of the octahedral Al^{3+} sites, continuing the spinel structure of the alumina with structurally similar Cr_2O_3. The formation of this structure would then have a stabilizing effect on the Cr^{3+} species (10). A similar model has been proposed for the growth of V_2O_5 on γ-alumina (32, 37). Upon recalcination at 550°C, Weckhuysen *et al.* (9, 10) observed that most of the Cr^{3+} was reoxidized to Cr^{6+}, while the isolated or dispersed Cr^{3+} resisted oxidation. This effect was also assigned to the stabilization of the Cr^{3+} species by the alumina support. The work of De Rossi *et al.* (13) supports the observation. Upon recalcination, they found that a small fraction of Cr^{3+} produced in the reductions could not be reoxidized on alumina, whereas on silica and zirconia systems the Cr was oxidized reversibly. They suggested that the Cr^{3+} species were less exposed on the surface of γ-alumina.

Consideration of our results in the light of the literature encourages us to propose the following growth mechanism. The ALE process ensures a high dispersion over the dehydroxylated alumina support and stabilizes Cr^{3+} even at low loadings of Cr. Even during the first cycle Cr^{3+} can be incorporated into sites on the spinel surface. Jacobs *et al.* (38) have shown that the surfaces of spinels, including γ-alumina, expose only the octahedral sites. The Cr^{3+} would thus easily be incorporated into just these sites, and it would still be visible to LEIS. Alternatively, or later in the growth, the spinel structure of the γ-alumina may be extended. The successive ALE sequences to increase the Cr loading ensure high dispersion, and with an air-treatment step after every $Cr(acac)_3$ sequence the Cr^{3+} is likely to be stabilized, resulting in a relatively high fraction of Cr in the oxidation state 3+ even without any reduction step. Because of strong chromia-alumina interaction, this stabilization makes the formation of Cr^{3+} irreversible. Chromium in oxidation state 6+ is probably stabilized on alumina as mono-, di-, or polychromate structures, depending on the Cr loading, similarly to impregnated catalysts (3). Hence, the oxidation step changes the bonding of Cr to the support from the monodentate species of type-$Cr(acac)_2$ to chromate species which are bound to the surface through more than one bond.

Catalytic Activity of Chromia/Alumina Catalysts

The measured increase in initial activity with chromium loading is in agreement with the findings of De Rossi *et al.* (13) and Gorritz *et al.* (18) in studies on the dehydrogenation of propane. De Rossi *et al.* measured increased activity for chromia/γ-alumina catalysts with a loading up to 1.0 Cr/nm^2, while Gorritz *et al.* observed the initial conversion to increase in a wider concentration range up to 4 wt% of Cr (3.3 Cr/nm^2). According to De Rossi *et al.*, the linear correlation that they found between dehydrogenation activity and Cr concentration indicates mononuclear chromium to be the active site. Our results are consistent with this conclusion, because even the low-loaded catalysts, in which dispersion presumably is at atomic level, were active. In other words, Cr did not need to be present in pairs or in greater ensembles in order to produce active catalysts. On the other hand, increasing coverage was not deleterious to the activity. An active Cr site or sites evidently can be formed in structures including more than one Cr atom.

In the work of Gorritz *et al.* (18) further increase of the loading from 4 wt% was accompanied by only a small increase in the activity, whereas in our work the activity continued to increase linearly after the monolayer coverage was exceeded. In other words, activity increased even though the Cr atoms were no longer all surface atoms. Evidently the continued increase in the activity can only be explained by higher reactivity per active site in the second layer or, if only part of the chromium monolayer surface species are active, by an increase in the number of active sites. The latter would mean that Cr in the second layer can be active and simultaneously it does not destroy the active site in the first layer. Since we studied only one data point above the monolayer, further speculation is not warranted.

The interesting feature of the catalytic behavior above monolayer coverage cannot wholly be explained by our present knowledge or on the basis of the literature. We are therefore carrying out experiments at still higher loadings, to shed light on these questions. Furthermore, catalysts prepared by ALE and impregnation techniques will be compared to study in detail the influence of the preparation method and oxidation state distribution on the dehydrogenation activity of the catalysts in detail.

CONCLUSIONS

The chemisorption of $Cr(acac)_3$ on γ-Al_2O_3 in the ALE process proved to be independent of the loading of Cr in repeated ALE sequences of $Cr(acac)_3$ and air. A saturation coverage of 0.8 Cr/nm^2 was found. We believe that the steric hindrance of the acac groups is the determining factor in the coverage, since the number of available binding sites is large. The ALE method resulted in a homogeneously distributed Cr coverage throughout the catalyst particles, even after seven ALE cycles. Surface area and pore volume measurements were in agreement with the weight increase of Cr.

Characterization of oxidized surfaces by LEIS showed a monolayer dispersion up to 4.5 Cr/nm^2 corresponding to six ALE cycles. A higher dispersion was reached for the ALE catalysts than reported in the literature for impregnated catalysts. The growth mechanism of Cr on γ-alumina sup-

port was different from that of NiO on alumina although an acetylacetonate compound was used as precursor in both systems. In the case of Ni, the formation of NiO agglomerates was observed by LEIS as early as the second ALE cycle.

XPS and UV-vis spectrophotometry showed that, from the first ALE sequence onwards, a significant amount of the Cr was in the Cr^{3+} oxidation state. We believe that, owing to its high dispersion on the dehydrated γ-alumina surface, the Cr could be easily stabilized and more easily than in wet-chemical methods where the stabilization occurs only after a few oxidation/reduction cycles. This stabilization could occur as Cr^{3+} diffused into the vacant octahedral Al^{3+} positions of the defect spinel structure of the support, or, alternatively, as a growth of Cr^{3+} species extending the γ-alumina spinel structure.

The activity in the dehydrogenation of *i*-butane to *i*-butene was measured both at low Cr concentrations and above monolayer coverage. At low Cr concentrations, the activity of samples in which Hacac and Hthd blocking agents were used to ensure high dispersion of the CrO_x species indicated that mononuclear Cr centers determine the catalytic activity. There was no decline in the rate of dehydrogenation when the monolayer coverage was exceeded; rather the activity continued to increase.

ACKNOWLEDGMENTS

Mirja Rissanen and Päivi Jokimies are thanked for the ALE processing and UV-vis spectrophotometric measurements. The help of Olli Jylhä, Ilkka Savolainen (XPS), Seppo Hornytzkyj (SEM/EDS), and Juha Vilhunen (XRD) working in the Scientific Services, Analytical Research of Neste Co. is also gratefully acknowledged. Arla Kytökivi, Arja Hakuli, and Jouni Meriläinen received financial support from the Academy of Finland, and Jean-Paul Jacobs from the Netherlands Foundation of Chemical Research (SON) and the Netherlands Organization for the Advancement of Scientific Research (NWO).

REFERENCES

1. Poole, C. P., and MacIver, D. S., *Adv. Catal.* **17**, 223 (1967) and references therein.
2. Vuurman, M. A., Stufkens, D. J., Oskam, A., Moulijn, J. A., and Kapteijn, F., *J. Mol. Catal.* **60**, 83 (1990).
3. Vuurman, M. A., Hardcastle, F. D., and Wachs, I. E., *J. Mol. Catal.* **84**, 193 (1993).
4. Vuurman, M. A., Wachs, I. E., Stufkens, D. J., and Oskam, A., *J. Mol. Catal.* **80**, 209 (1993).
5. Kim, D. S., and Wachs, I. E., *J. Catal.* **142**, 166 (1993).
6. Turek, A. M., Wachs, I. E., and DeCanio, E., *J. Phys. Chem.* **96**, 5000 (1992).
7. Wachs, I. E., Deo, G., Vuurman, M. A., Hu, H., Kim, D. S., and Jehng, J.-M., *J. Mol. Catal.* **82**, 443 (1993).
8. Weckhuysen, B. M., De Ridder, L. M., and Schoonheydt, R. A., *J. Phys. Chem.* **97**, 4756 (1993).
9. Weckhuysen, B. M., Verberckmoes, A. A., Buttiens, A. L., and Schoonheydt, R. A., *J. Phys. Chem.* **98**, 579 (1994).
10. Weckhuysen, B. M., De Ridder, L. M., Grobet, P. J., and Schoonheydt, R. A., *J. Phys. Chem.* **99**, 320 (1995).
11. Fouad, N. E., Knözinger, H., Zaki, M. I., and Mansour, S. A. A., *Z. Phys. Chem.* **171**, 75 (1991).
12. Fouad, N. E., Knözinger, H., and Zaki, M. I., *Z. Phys. Chem.* **186**, 231 (1994).
13. De Rossi, S., Ferraris, G., Fremiotti, S., Garrone, E., Ghiotti, G., Campa, M. C., and Indovina, V., *J. Catal.* **148**, 36 (1994).
14. Cordischi, D., Indovina, V., and Occhiuzzi, M., *Appl. Surf. Sci.* **55**, 233 (1992).
15. Rahman, A., Mohamed, M. H., Ahmed, M., and Aitani, A. M., *Appl. Catal. A* **121**, 203 (1995).
16. Köhler, S., dissertation, Ruhr-Universität, Bochum, Germany, 1994.
17. Köhler, S., Reiche, M., Frobel, C., and Baerns, M., *Stud. Surf. Sci. Catal.* **91**, 1009 (1995).
18. Gorriz, O. F., Cortés Corberán, V., and Fierro, J. L. G., *Ind. Chem. Eng. Res.* **31**, 2670 (1992).
19. Scierka, S. J., Houalla, M., Proctor, A., and Hercules, D. M., *J. Phys. Chem.* **99**, 1537 (1995).
20. Suntola, T., *Mater. Sci. Rep.* **4**, 261 (1989).
21. Suntola, T., *in* "Handbook of Crystal Growth" (D. T. J. Hurle, Ed.), Vol. 3, part B, p. 601. Elsevier Science, Amsterdam, 1994.
22. Lakomaa, E.-L., *Appl. Surf. Sci.* **75**, 185 (1994).
23. Jacobs, J,-P., Reintjes, J. G. H., Brongersma, H. H., Lindfors, L. P., and Jylhä, O., *Catal. Lett.* **25**, 315 (1994).
24. Lindblad, M., Lindfors, L. P., and Suntola, T., *Catal. Lett.* **27**, 323 (1994).
25. Haukka, S., Lakomaa, E.-L., and Suntola, T., *Appl. Surf. Sci.* **75**, 220 (1994).
26. Haukka, S., Lakomaa, E.-L., and Suntola, T., *Appl. Surf. Sci.* **82/83**, 548 (1994).
27. Haukka, S., and Saastamoinen, A., *Analyst* **117**, 1381 (1992).
28. Brongersma, H. H., Groenen, P. A. C., and Jacobs, J.-P., *in* "Science of Ceramic Interfaces II" (J. Nowotny, Ed.), Vol. 81, p. 113. Mat. Sci. Monographs, Elsevier Science, Amsterdam, 1994.
29. Saarinen, P., and Kauppinen, J., *Appl. Spectrosc.* **45**, 953 (1991).
30. Hakuli, A., Kytökivi, A., Lakomaa, E.-L., and Krause, O., *Anal. Chem.* **67**, 1881 (1995).
31. Grünert, W., Shpiro, E. S., Feldhaus, R., Anders, K., Antoshin, G. V., and Minachev, Kh.M., *J. Catal.* **100**, 138 (1986).
32. Jacobs, J.-P., Van Leerdam, G. C., and Brongersma, H. H., *in* "Fundamental Aspects of Heterogeneous Catalysis Studied by Particle Beams" (H. H. Brongersma and R. A. van Santen, Eds.), p. 339. Plenum, New York, 1991.
33. Nelson, G. C., *J. Vac. Sci. Technol. A* **4**, 1567 (1986).
34. Drimal, J., and Koksa, V., in preparation.
35. Jagannathan, K., Srinivasan, A., and Rao, C. N. R., *J. Catal.* **69**, 418 (1981).
36. Kozłowski, R., *Bull. Polish Acad. Sci. Chem.* **35**, 365 (1986).
37. Stobbe-Kreemers, A. W., van Leerdam, G. C., Jacobs, J.-P., Brongersma, H. H., and Scholten, J. J. F., *J. Catal.* **152**, 130 (1995).
38. Jacobs, J.-P., Maltha, A., Reintjes, J. G. H., Drimal, J., Ponec, V., and Brongersma, H. H., *J. Catal.* **147**, 294 (1994).